Published online: September 30, 2019

IMR Press

Original Research

Dl-3-n-butylphthalide inhibits phenytoin-induced neuronal apoptosis in rat hippocampus and cerebellum

Junmin Chen[1,†], Na Liu[1,2,†], Xiaopeng Wang[1,*], Yanying Zhao[1], Junna He[1], Lan Yang[1], Qian Sun[1], Jing Zhao[1], Linjing Wang[3] and Lei Chen[3]

[1]*Department of Neurology, Second Hospital of Hebei Medical University, 215 Hepingxi Road, Shijiazhuang 050000, Hebei, P. R. China*

[2]*Department of Neurology, Affiliated Hospital of Hebei University, 212 East Yuhua Road, Baoding 071000, Hebei, P. R. China*

[3]*Department of Neurology, People's Hospital in Shijiazhuang, 36 Fanxi Road, Shijiazhuang 050000, Hebei, P. R. China*

†These authors contributed equally.
*Correspondence: xiaopengwangcn@126.com (Xiaopeng Wang)

DOI:10.31083/j.jin.2019.03.174

Rats were divided into six groups: sham/control, Dl-3-n-butylphthalide, P1 (low phenytoin, 100 mg/kg), P2 (high phenytoin, 200 mg/kg), NP1 (Dl-3-n-butylphthalide 80 mg/kg, phenytoin 100 mg/kg), NP2 (Dl-3-n-butylphthalide 80 mg/kg, phenytoin 200 mg/kg). Hematoxylin/eosin and Nissl staining showed that, compared to the sham/control group, the Dl-3-n-butylphthalide group had no obvious hippocampal and cerebellar neuron loss, but there was a significant neuron loss in the P1 and P2 groups ($P < 0.05$), which was more obvious in the P2 group ($P < 0.05$). The positive expression of Bax and Bcl-2 proteins in hippocampal and cerebellar neurons was not significantly different between sham and Dl-3-n-butylphthalide groups; however, compared to sham, Bax expression was significantly increased and Bcl-2 was significantly decreased in the hippocampal and cerebellar neurons of rats in both P1 and P2 groups ($P < 0.05$), being more obvious in the P2 group ($P < 0.05$). Furthermore, the administration of Dl-3-n-butylphthalide attenuated the deleterious effects of phenytoin ($P < 0.05$). Our results indicate that phenytoin causes apoptosis of hippocampal and cerebellar neurons in rats in a dose-dependent manner, with the effect of a higher dose being more obvious, whereas, Dl-3-n-butylphthalide inhibits the phenytoin-induced apoptosis of neurons and has a neuroprotective role.

Keywords

Dl-3-n-butylphthalide; apoptosis; cerebellar neurons; hippocampal neurons; phenytoin; Bax protein; Bcl-2 protein; neuropharmacology; immunohistochemistry

1. Introduction

Abnormal discharge of the brain, thalamic cortical system, and upper midbrain neurons is the root cause of epilepsy, but its specific pathogenesis remains unclear (Baldassari et al., 2019; Devinsky et al., 2013).

Studies have shown that neuronal apoptosis is a key event in the pathogenesis of epilepsy and can play a role in reducing brain damage after epilepsy by inhibiting apoptosis (Dai et al., 2018; Singh et al., 2019).

Phenytoin (PHT) is a common antiepileptic drug with a narrow therapeutic spectrum. Numerous studies have shown that PHT not only has antiepileptic properties but also may induce neuronal apoptosis and thus damage the nervous system (Kaushal et al., 2016). Long-term use or an overdose of PHT may cause irreversible cerebellar atrophy (Fang et al., 2016; Singh et al., 2019; Ye et al., 2018). Therefore, preventing neuronal apoptosis is essential for the treatment of epilepsy.

Dl-3-n-butylphthalide (NBP) belongs to a new class of drugs that protect nerve cells and inhibit apoptosis and is used in the treatment of heart and cerebrovascular diseases (He et al., 2017; Lv et al., 2018). Whether NBP can inhibit PHT-induced apoptosis of nerve cells in the treatment of epilepsy is still unclear. Bcl-2 is an anti-apoptotic protein that regulates the apoptotic pathway and prevents cell death. Alternatively, Bax is a pro-apoptotic protein of the Bcl-2 family. Apoptosis can be detected by measuring Bax and Bcl-2 expression (He et al., 2016; Teymournejad et al., 2017; Zhang et al., 2016).

Given the neurotoxic side effects of PHT, we investigate whether NBP plays a protective effect on the PHT-induced apoptosis of neurons. To this end, the morphology and quantity of apoptotic cells were assessed in the hippocampus and cerebellum by hematoxylin and eosin (H&E) and Nissl staining. Expression levels of the anti-apoptotic protein Bcl-2 and the pro-apoptotic protein Bax in the hippocampus and cerebellum were also detected by immunohistochemistry.

Journal of Integrative Neuroscience

2. Materials and methods

2.1 Animal studies

Male Sprague Dawley rats (8-10 weeks old, 170 ± 20 g) were provided by the animal experimental center of Hebei medical university (certificate No.: 1409045) and housed in the neurology laboratory of second hospital of Hebei medical university. All animals were kept at a constant temperature of 22 ± 1 ℃ with a 12-hour light/dark cycle and given access to food and water *ad libitum*. All animal care and experimental procedures complied with regulations of the animal care and management committee of the second hospital of Hebei medical university (permit No. HMUSHC-130318) and the ARRIVE guidelines for reporting experiments (Kilkenny et al., 2010; McGrath et al., 2010).

2.2 Drug administration and experimental protocol

NBP and PHT were purchased from CSPC Pharmaceutical Company (CSPC Pharmaceutical Group Limited, Shijiazhuang, China). Rats were randomly divided into groups of six using a random number table generated with SPSS software version 21.0, (IBM Corporation, Armonk, NY, USA). An effective dose of PHT is between 200 mg/day and 500 mg/day. The high and low doses of PHT in rats were approximately 200 mg/kg/day and 100 mg/kg/day, respectively, which are 25 times higher than the normal effective therapeutic dose for adults of standard bodyweight. The dose used for NBP was 80 mg/kg/day (Qi et al., 2018). Normal saline was used for equal dose feeding. The specific groups tested were sham (same volume of normal saline was administered), NBP (NBP 80 mg/kg/day), P1 (low PHT, 100 mg/kg/day), P2 (high PHT, 200 mg/kg/d), NP1 group (NBP 80 mg/kg/d, PHT 100 mg/kg/d) and NP2 (NBP 80 mg/kg/d, PHT 200 mg/kg/day). The two drugs were administered between 09: 00 am and 11: 00 am daily for 30 days. PHT was administered first, and after 30 minutes it was followed by NBP.

2.3 Specimen preparation

Animals underwent intracardiac perfusion with saline quickly followed by cold 4% paraformaldehyde in 0.1 M phosphate-buffered saline (PBS). The brain was then immersed in 4% paraformaldehyde (for at least 24 hours), dehydrated in serial dilutions of ethanol and embedded in paraffin. Brain tissues were cut into 5 μm sections using a rotary microtome (Leica® RM1850, Germany) and these sections were used for H&E and Nissl staining.

2.4 Hematoxylin and eosin staining

After the brain sections were routinely dewaxed, hydrated, and stained in hematoxylin solution for five minutes, they were decolorized in 1% hydrochloric acid ethanol for 10 seconds. Sections were then stained with eosin for two minutes. After sealing the slides with a neutral resin, they were observed under light microscopy (Olympus BH-Z, Japan).

2.5 Nissl staining

Paraffin sections were incubated at 65 ℃ for 10 minutes, dewaxed and washed with water. Sections were then hydrated in 0.1% cresyl violet for six minutes, then dehydrated in serial dilutions of ethanol and cleaned with xylene. The slides were then viewed and photographed under the light microscope.

2.6 Immunohistochemical staining

Brain sections were blocked in 3% H_2O_2 and 3% normal goat serum and incubated with rabbit polyclonal antibody for Bax (1 : 100, Zhongshan Biology Technology Company, Beijing, China) and Bcl-2 (1 : 100, Zhongshan Biology Technology Company, Beijing, China) in 0.01 M PBS overnight at 4 °C. The next day, sections were heated for 45 minutes in a 37 °C incubator and washed with 0.01 M PBS. After incubation with goat anti-rabbit horseradish peroxidase secondary antibody, sections were stained with DAB chromogen and counterstained with hematoxylin. Finally, slides were analyzed by an optical microscope. Six brain sections were randomly selected from each rat, and the average optical density (AOD) values of cells positive for Bax and Bcl-2 obtained.

2.7 Statistical analysis

Statistical analysis was performed with SPSS 21.0 software. The AOD value was expressed as mean ± SD. The data were first tested for normality, and Levene's test was used to assess the uniformity of the variance. Statistical comparisons were performed by one-way ANOVA, followed by the least significant difference test for multiple comparisons. A value of $P < 0.05$ was considered statistically significant.

3. Results

3.1 Hematoxylin and eosin staining of hippocampal and cerebellar neurons in each experimental group

Hippocampal neurons from the sham and NBP groups showed a clear cell structure, and an organized cellular pattern and H&E staining showed no obvious pathological changes. The nucleus was round or elliptical, the nucleolus clear and morphology normal. Compared with the sham group, neurons in the P1 and P2 groups were sparsely arranged, their outline was blurred, and the nucleus was condensed and surrounded by vacuoles, this was more marked in the P2 group. In NP1 and NP2 groups, NBP treatment reduced PHT-induced cell damage (Fig. 1A).

H&E staining showed no obvious pathological changes in cerebellar neurons in the NBP group compared with sham: cell structure was clear, and the cellular arrangement was organized. The nucleus was round or elliptical, the nucleolus was clear, and the morphology was normal. Compared with the sham group, the neurons in the P1 and P2 groups were sparsely arranged, the outline was blurred, the nucleus was condensed, and the surrounding vacuoles were formed, which was more marked in the P2 group. In NP1 and NP2 groups, NBP treatment reduced PHT-induced cell damage (Fig. 1B).

3.2 Nissl staining observation of hippocampal and cerebellar neurons in rats of each experimental group

Nissl staining showed that hippocampal neurons from the sham and NBP groups were stained light blue and their contour was intact. However, in the P1 and the P2 groups, the occurrence of shrunken somata and pyknotic nuclei revealed PHT-induced neuron damage, which was more severe in the P2 group. In the NP1 and NP2 groups, NBP treatment decreased the occurrence of shrunken somata and PHT-induced pyknotic (Fig. 2A).

Nissl staining showed that the cerebellar neurons from the sham and NBP groups were stained light blue and their contour was intact. However, in the P1 and the P2 groups, the occurrence

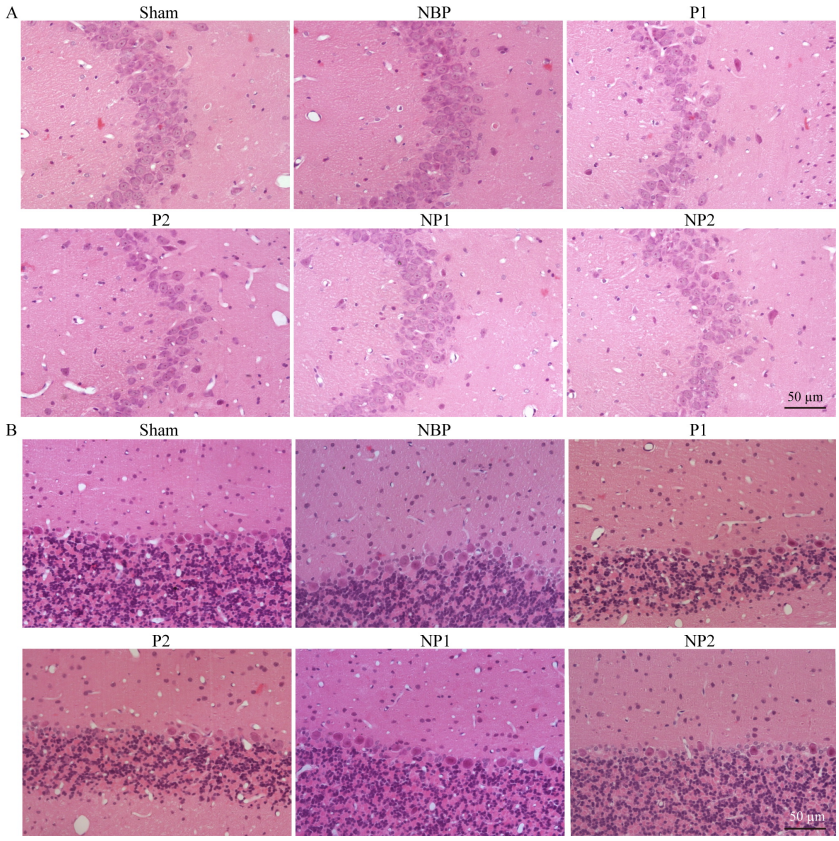

Figure 1. Hematoxylin and eosin staining. Staining of A: Hippocampal and B: Cerebellar regions in sham, NBP, P1, P2, NP1, and NP2 groups. A: Hippocampal neurons from the sham and NBP groups showed a clear cell structure and an organized cellular pattern. Hippocampal neurons in the P1 and P2 groups were sparsely arranged, their outline was blurred, and the nucleus was condensed and surrounded by vacuoles. In the NP1 and NP2 groups, NBP treatment reduced PHT-induced cell damage. B: Cerebellar neurons from the sham and NBP groups showed a clear cell structure and an organized cellular pattern. Cerebellar neurons in the P1 and P2 groups were sparsely arranged, their outline was blurred, and the nucleus was condensed and surrounded by vacuoles. In the NP1 and NP2 groups, NBP treatment reduced PHT-induced cell damage.

of shrunken somata and pyknotic nuclei revealed neuron damage induced by PHT, which was more severe in the P2 group. In the NP1 and NP2 groups, NBP treatment decreased the occurrence of shrunken somata and pyknotic nuclei induced by PHT (Fig. 2B).

3.3 Positive expression of Bax protein in rat hippocampal and cerebellar neurons

The positive expression of Bax protein is observed as brown color particles that were mainly distributed in the cell membrane and cytoplasm. Compared with the sham group, there was no significant increase in either Bax-positive cells or optical density in the hippocampal and cerebellar neurons of the NBP group. In P1 and P2 groups, both Bax-positive cells and optical density in hippocampal neurons were both significantly increased when compared with the sham group ($P = 0.038$, P1 group *vs*. sham group; $P = 0.008$, P2 group *vs*. sham group; n = 6 each group). In P1 and P2 groups, Bax-positive cells and optical density were significantly increased in the cerebellar neurons compared with the sham group ($P = 0.033$, P1 group *vs*. sham group; $P = 0.007$, P2 group *vs*. sham group; n = 6 each group). A relative higher optical density was observed in the P2 group compared to the P1 group, suggesting that neuronal damage caused by PHT may be dose-related ($P = 0.012$, P2 group *vs*. P1 group in hippocampal neurons; $P = 0.010$, P2 group *vs*. P1 group in cerebellar neurons; n = 6 each group). NBP treatment significantly attenuated both the enhancing effects of PHT on Bax-positive cells and optical density in hippocampal and cerebellar neurons ($P = 0.026$, NP1 group *vs*. P1 group in hippocampal neurons; $P = 0.013$, NP2 group *vs*. P2 group in hippocampal neurons; $P = 0.023$, NP1 group *vs*. P1 group in cerebellar neurons; $P = 0.018$, NP2 group *vs*. P2 group in cerebellar neurons; n = 6 each group) (Figs. 3A-D).

3.4 Positive expression of Bcl-2 protein in rat hippocampal and cerebellar neurons

The positive expression of Bcl-2 protein was observed as brown, heavily stained granules, mainly distributed in the cell membrane and cytoplasm.

Compared with the sham group, there was no significant decrease in either Bcl-2-positive cells or optical density in the hippocampal and cerebellar neurons of the NBP group. In the P1 and P2 groups, the Bcl-2-positive cells and optical density were both significantly decreased in the hippocampal and cerebellar neurons when compared with the sham group ($P < 0.0005$, P1 group *vs*. sham group in hippocampal neurons; $P < 0.0005$, P2 group *vs*. sham group in hippocampal neurons; $P < 0.0005$, P1 group *vs*. sham group in cerebellar neurons; $P < 0.0005$, P2 group *vs*. sham

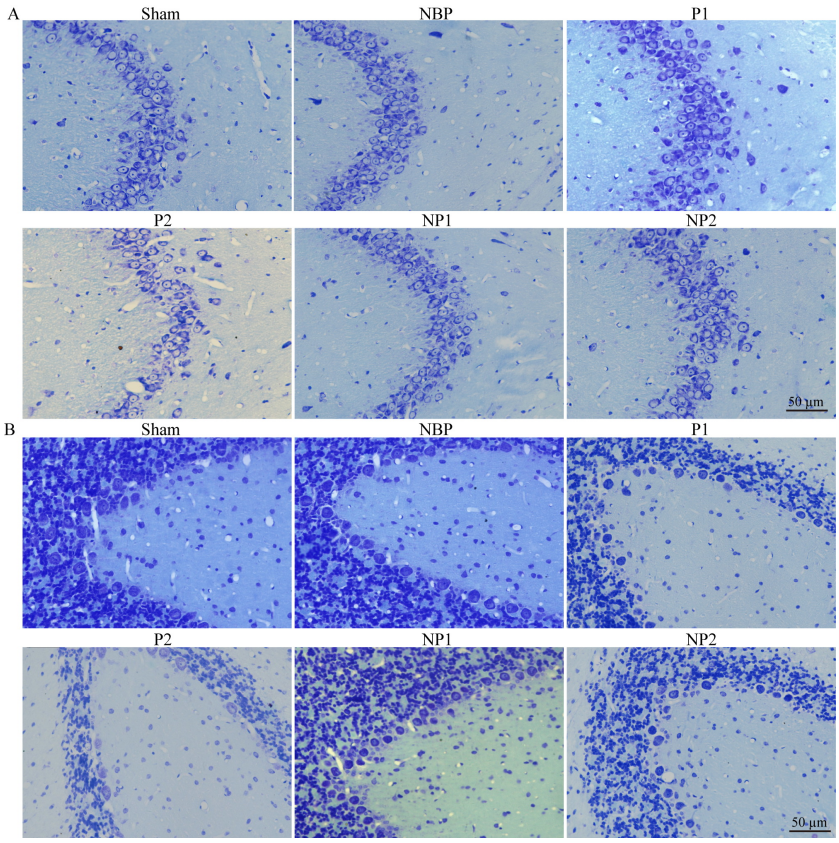

Figure 2. Nissl staining. Staining of A: Hippocampal and B: Cerebellar regions in sham, NBP, P1, P2, NP1, and NP2 groups. A: Hippocampal neurons from the sham and NBP groups were stained light blue, and their contour was intact. In the P1 and the P2 groups, the occurrence of shrunken somata and pyknotic nuclei. In the NP1 and NP2 groups, NBP treatment decreased the occurrence of shrunken somata and PHT-induced pyknotic. B: Cerebellar neurons from the sham and NBP groups were stained light blue, and their contour was intact. In the P1 and the P2 groups, the occurrence of shrunken somata and pyknotic nuclei. In the NP1 and NP2 groups, NBP treatment decreased the occurrence of shrunken somata and pyknotic nuclei induced by PHT.

group in cerebellar neurons; n = 6 each group). A relatively lower optical density was observed for the P2 group when compared to the P1 group, suggesting that neuronal damage caused by PHT may be dose-related ($P = 0.020$, P2 group *vs*. P1 group in hippocampal neurons; $P = 0.032$, P2 group *vs*. P1 group in cerebellar neurons; n = 6 each group). When compared with the P1 group, the Bcl-2-positive cells and optical density were both significantly decreased for the hippocampal and cerebellar neurons of the NP1 group ($P < 0.0005$, NP1 group *vs*. P1 group in hippocampal neurons; $P < 0.0005$, NP1 group *vs*. P1 group in cerebellar neurons; n = 6 each group). When compared with the P2 group, NBP treatment significantly attenuated the PHT-induced decrease in both Bcl-2-positive cells and the optical density of hippocampal and cerebellar neurons ($P < 0.0005$, NP2 group *vs*. P2 group in hippocampal neurons; $P < 0.0005$, NP2 group *vs*. P2 group in cerebellar neurons; n = 6 each group) (Figs. 4A-D).

4. Discussion

Antiepileptic drugs for the treatment of seizures are accompanied by adverse effects, such as cognitive impairment, microcephaly, and congenital disabilities. The cause of the adverse effects of antiepileptic drugs is unknown (Fang et al., 2016; Landmark and Patsalos, 2010; Ye et al., 2018). PHT is a common antiepileptic drug, but its therapeutic spectrum is narrow (Appleton and Gill, 2003). Some studies have shown that PHT can cause neuronal damage, in the nervous system (Bittigau et al., 2002; Guimarães et al., 2010; Zhao et al., 2003). Here, the effects of high and low doses of PHT on neuronal damage of the hippocampus and cerebellum in rats were studied. H&E staining showed that hippocampal and cerebellar neurons of rats treated with high and low doses of PHT were damaged compared with a sham group. This indicates that PHT has adverse effects and damages neurons of the central nervous system.

The mechanism of toxicity by which PHT induces neuronal damage is unclear. Some studies have shown that PHT causes neuronal apoptosis (Bittigau et al., 2002; Zhao et al., 2003). Apoptosis refers to a form of cell death controlled by genes, regulates the development of the body and maintains the stability of the internal environment (Abeti et al., 2016; Chen et al., 2017; Gahl et al., 2016; Han et al., 2018). Studies have shown that neuronal apoptosis is a key event in the pathogenesis of epilepsy, cerebral ischemia and other diseases (Abiega et al., 2016; Dai et al., 2018; Li et al., 2017; Singh et al., 2019). In this work, the effect of high and low doses of PHT on the apoptosis of cells of the rat hippocampus and cerebellum was studied. Nissl staining in rat hippocampal and cerebellar neurons treated with high and low doses of PHT showed apopto-

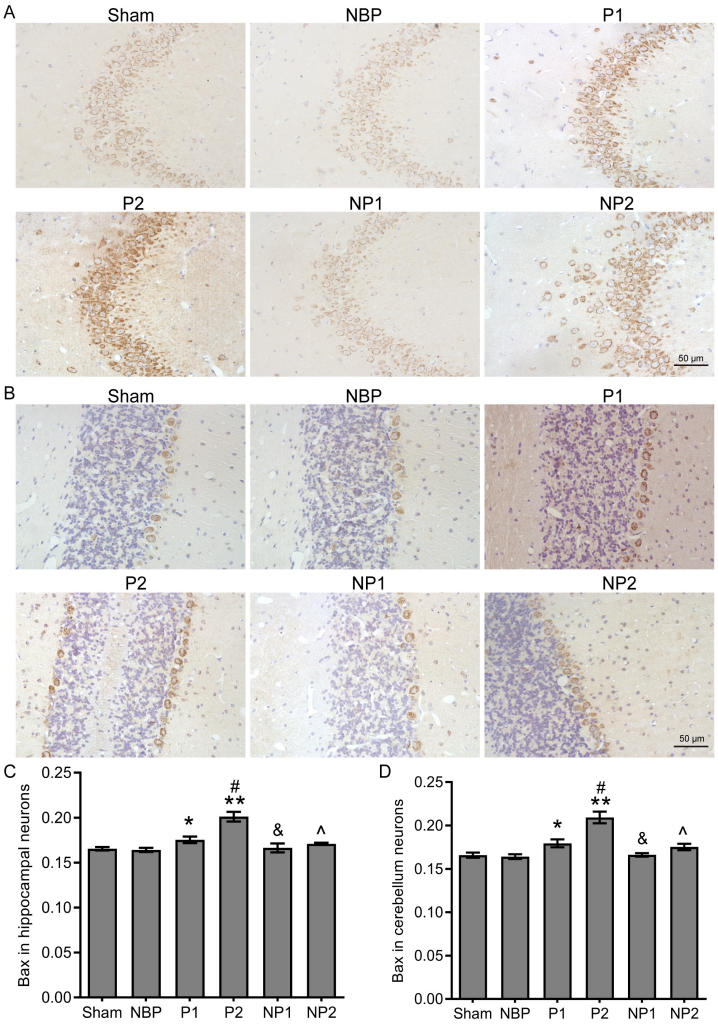

Figure 3. Immunohistochemical staining of Bax in rat hippocampus and cerebellum neurons. Bax positive cell expression in A: Hippocampus and B: Cerebellum of sham, NBP, P1, P2, NP1, and NP2 groups. Mean average optical density (Bax) in C: Hippocampal neurons of each group ($*P = 0.038$, P1 *vs.* sham; $**P = 0.008$, P2 *vs.* sham; $\#P = 0.012$, P2 *vs.* P1; $\&P = 0.026$, NP1 *vs.* P1; $\hat{}P = 0.013$, NP2 *vs.* P2; n = 6, one-way ANOVA with LSD test) and D: Cerebellar neurons of each group ($*P = 0.033$, P1 *vs.* sham; $**P = 0.007$, P2 *vs.* sham; $\#P = 0.010$, P2 *vs.* P1; $\&P = 0.023$, NP1 *vs.* P1; $\hat{}P = 0.018$, NP2 *vs.* P2; n = 6, one-way ANOVA with LSD test).

sis when compared with the sham group. Compared with the sham group, there was a significant decrease in both Bcl-2-positive cells and optical density in the hippocampal and cerebellar neurons of rats treated with high and low doses of PHT, while Bax-positive cells and their optical density were both significantly increased. This suggests that high and low doses of PHT play a role in the apoptosis of rat hippocampal and cerebellar nerve cells, while a high dose of PHT causes more serious neuronal apoptosis.

Many studies suggest that NBP promotes the recovery of neurological function after an ischemic stroke and reduces the volume of cerebral infarction by inhibiting apoptosis (Abdoulaye and Guo, 2016; Chang and Wang, 2003; Wen et al., 2016). In cortical neuron oxygen-glucose deprivation and permanent middle cerebral artery occlusion animal model experiments, NBP attenuates neuronal apoptosis induced by serum deprivation and reduces the expression of apoptosis-inducing factor in the ischemic penumbra, thereby protecting ischemic brain tissue (Li et al., 2010). In bone marrow stem cell oxidative stress injury models, NBP attenuates apoptosis by up-regulating both the Bax/Bcl-2 ratio, and caspase-3 expression levels (Sun et al., 2012). In the oxygen-glucose deprivation model of brain microvascular endothelial cells, NBP down-regulates both the expression of caspase-3 and apoptosis by up-regulating Bcl-2 expression (Yang et al., 2012). Whether NBP can alleviate PHT- induce neuronal apoptosis remains unclear. We had shown that NBP could alleviate PHT-induced neuronal damage to the rat hippocampus and cerebellum.

Additionally, it was found that NBP attenuates PHT-induced apoptosis of rat hippocampal and cerebellar neurons by increasing the expression of the anti-apoptotic protein Bcl-2 and decreasing expression of the pro-apoptotic protein Bax. This indicates that NBP alleviates the adverse reactions induced by PHT. Different therapeutic doses of PHT cause dose-dependent apoptosis of hippocampal and cerebellar neurons in rats, as apoptosis is more evident in the high dose group while NBP inhibits this apoptosis and has a neuroprotective role.

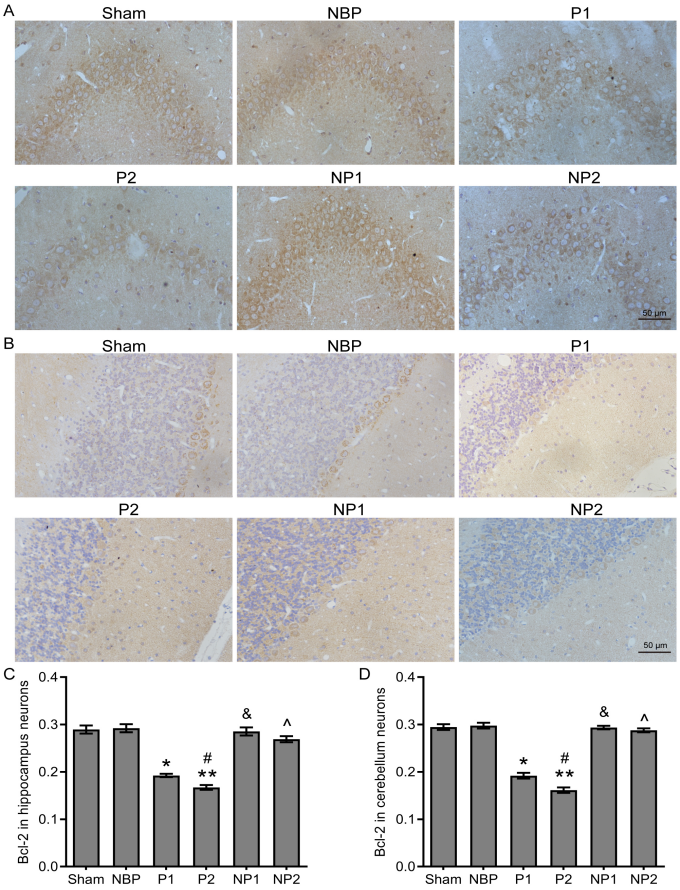

Figure 4. Immunohistochemical staining of Bcl-2 in rat hippocampal and cerebellar neurons. Bcl-2 positive cell expression of A: Hippocampal and B: Cerebellar neurons in sham, NBP, P1p, P2, NP1, and NP2 groups. Mean average optical density (Bcl-2) in C: Hippocampal neurons of each group ($*P \leq 0.0005$, P1 *vs*. sham; $**P \leq 0.0005$, P2 *vs*. sham; $\#P = 0.020$, P2 *vs*. P1; $\&P \leq 0.0005$, NP1 *vs*. P1; $\hat{}P \leq 0.0005$, NP2 *vs*. P2; n = 6, one-way ANOVA with LSD test) and D: Cerebellar neurons of each group ($*P \leq 0.0005$, P1 *vs*. sham; $**P \leq 0.0005$, P2 *vs*. sham; $\#P = 0.032$, P2 *vs*. P1; $\&P \leq 0.0005$, NP1 *vs*. P1; $\hat{}P \leq 0.0005$, NP2 *vs*. P2; n = 6, one-way ANOVA with LSD test).

Acknowledgment

We thank Academician of China Engineering Academy Chunyan Li Ph.D. and Weiping Wang Ph.D. for their equipment and technical assistance.

Conflicts of interest

The authors declare no conflict of interest.

Submitted: June 10, 2019
Accepted: September 03, 2019
Published: September 30, 2019

References

Abdoulaye, I. A., and Guo, Y. J. (2016) A review of recent advances in neuroprotective potential of 3-N-Butylphthalide and its derivatives. *Biomed Research International* **2016**, 5012341.

Abeti, R., Parkinson, M. H., Hargreaves, I. P., Angelova, P. R., Sandi, C., Pook, M. A., Giunti, P. and Abramov, A. Y. (2016) Mitochondrial energy imbalance and lipid peroxidation cause cell death in Friedreich's ataxia. *Cell Death & Disease* **7**, e2237.

Abiega, O., Beccari, S., Diaz-Aparicio, I., Nadjar, A., Layé, S., Leyrolle, Q., Gómez-Nicola, D., Domercq, M., Pérez-Samartín, A., Sánchez-Zafra, V., Paris, I., Valero J., Savage J. C., Hui C. W., Tremblay M. È., Deudero J. J., Brewster A. L., Anderson, A. E., Zaldumbide, L., Galbarriatu, L., Marinas, A., Vivanco, M. D., Matute, C., Maletic-Savatic, M., Encinas, J. M. and Sierra, A. (2016) Neuronal hyperactivity disturbs ATP microgradients, impairs microglial motility, and reduces phagocytic receptor expression triggering apoptosis/microglial phagocytosis uncoupling. *PLOS Biology* **14**, e1002466.

Appleton, R. E. and Gill, A. (2003) Adverse events associated with intravenous phenytoin in children: a prospective study. *Seizure* **12**, 369-372.

Baldassari, S., Picard, F., Verbeek, N. E., van Kempen, M., Brilstra, E. H., Lesca, G., Conti, V., Guerrini, R., Bisulli, F., Licchetta, L., Pippucci, T., Tinuper, P., Hirsch, E., de Saint Martin, A., Chelly, J., Rudolf, G., Chipaux, M., Ferrand-Sorbets, S., Dorfmüller, G., Sisodiya, S., Balestrini, S., Schoeler, N., Hernandez-Hernandez, L., Krithika, S., Oegema, R., Hagebeuk, E., Gunning, B., Deckers, C., Berghuis, B., Wegner, I., Niks, E., Jansen, F.E., Braun, K., de Jong, D., Rubboli, G., Talvik, I., Sander, V., Uldall, P., Jacquemont, M.L., Nava, C., Leguern, E., Julia, S., Gambardella, A., d'Orsi, G., Crichiutti, G., Faivre, L., Darmency, V., Benova, B., Krsek, P., Biraben, A., Lebre, A. S., Jennesson, M., Sattar, S., Marchal, C., Nordli, D. R., Lindstrom, K., Striano, P., Lomax, L. B., Kiss, C., Bartolomei, F., Lepine, A. F., Schoonjans, A. S., Stouffs, K., Jansen, A., Panagiotakaki, E., Ricard-Mousnier, B., Thevenon, J., de Bellescize, J., Catenoix, H., Dorn, T., Zenker, M., Müller-Schlüter, K., Brandt, C., Krey, I., Polster, T., Wolff, M., Balci, M., Rostasy, K., Achaz, G., Zacher, P., Becher, T., Cloppenborg, T., Yuskaitis, C. J., Weckhuysen, S., Poduri, A., Lemke, J. R., Møller, R. S. and Baulac, S. (2019) The landscape of epilepsy-related GATOR1 variants. *Genetics in Medicine* **21**, 398-408.

Bittigau, P., Sifringer, M., Genz, K., Reith, E., Pospischil, D., Govindarajalu, S., Dzietko, M., Pesditschek, S., Mai, I., Dikranian, K., Olney, J. W. and Ikonomidou, C. (2002) Antiepileptic drugs and apoptotic neurodegeneration in the developing brain. *Proceedings of the National Academy of Sciences of the United States of America* **99**, 15089-15094.

Boatright, K. M. and Salvesen, G. S. (2003) Mechanisms of caspase activation. *Current Opinion in Cell Biology* **15**, 725-731.

Chang, Q. and Wang, X. L. (2003) Effects of chiral 3-n-butylphthalide on apoptosis induced by transient focal cerebral ischemia in rats. *Acta Pharmacologica Sinica* **24**, 796-804.

Chen, J., Wang, Y. X., Dong, M. Q., Zhang, B., Luo, Y., Niu, W. and Li, Z. C. (2017) Reoxygenation Reverses Hypoxic Pulmonary Arterial Remodeling by Inducing Smooth Muscle Cell Apoptosis via Reactive Oxygen Species-Mediated Mitochondrial Dysfunction. *Journal of the American Heart Association* **6**, e005602.

Dai, H., Wang, P., Mao, H., Mao, X., Tan, S. and Chen, Z. (2018) Dynorphin activation of kappa opioid receptor protects against epilepsy and seizure-induced brain injury via PI3K/Akt/Nrf2/HO-1 pathway. *Cell Cycle* 1-12.

Devinsky, O., Schein, A. and Najjar, S. (2013) Epilepsy associated with systemic autoimmune disorders. *Epilepsy Currents* **13**, 62-68.

Fang, Z., Chen, S., Qin, J., Chen, B., Ni, G., Chen, Z., Zhou, J., Li, Z., Ning, Y., Wu, C. and Zhou, L. (2016) Pluronic P85-coated poly (butylcyanoacrylate) nanoparticles overcome phenytoin resistance in P-glycoprotein overexpressing rats with lithium-pilocarpine-induced chronic temporal lobe epilepsy. *Biomaterials* **97**, 110-121.

Gahl, R. F., Dwivedi, P. and Tjandra, N. (2016) Bcl-2 proteins bid and bax form a network to permeabilize the mitochondria at the onset of apoptosis. *Cell Death & Disease* **7**, e2424.

Guimarães, J. and Ribeiro, J. A. (2010) Pharmacology of antiepileptic drugs in clinical practice. *Neurologist* **16**, 353-357.

Han, Y. Q., Ming, S. L., Wu, H. T., Zeng, L., Ba, G., Li, J., Lu, W. F., Han, J., Du, Q. J., Sun, M. M., Yang, G. Y., Wang, J. and Chu, B. B. (2018) Myostatin knockout induces apoptosis in human cervical cancer cells via elevated reactive oxygen species generation. *Redox Biology* **19**, 412-428.

He, J., Ji, X., Li, Y., Xue, X., Feng, G., Zhang, H., Wang, H. and Gao, M. (2016) Subchronic exposure of benzo(a)pyrene interferes with the expression of Bcl-2, Ki-67, C-myc and p53, Bax, Caspase-3 in subregions of cerebral cortex and hippocampus. *Experimental and Toxicologic Pathology* **68**, 149-156.

He, Z., Zhou, Y., Huang, Y., Wang, Q., Zheng, B., Zhang, H., Li, J., Liu, Y., Wu, F., Zhang, X., Tong, S., Wang, M., Wang, Z., He, H., Xu, H. and Xiao, J. (2017) Dl-3-n-butylphthalide improves functional recovery in rats with spinal cord injury by inhibiting endoplasmic reticulum stress-induced apoptosis. *American Journal of Translational Research* **9**, 1075-1087.

Kaushal, S., Tamer, Z., Opoku, F. and Forcelli, P. A. (2016) Anticonvulsant drug-induced cell death in the developing white matter of the rodent brain. *Epilepsia* **57**, 727-734.

Kilkenny, C., Browne, W., Cuthill, I. C., Emerson, M. and Altman, D. G. (2010) Animal research: reporting in vivo experiments: the ARRIVE guidelines. *British Journal of Pharmacology* **160**, 1577-1579.

Landmark, C. J. and Patsalos, P. N. (2010) Drug interactions involving the new second- and third-generation antiepileptic drugs. *Expert Review of Neurotherapeutics* **10**, 119-140.

Li, J., Li, Y., Ogle, M., Zhou, X., Song, M., Yu, S. P. and Wei, L. (2010) DL-3-n-butylphthalide prevents neuronal cell death after focal cerebral ischemia in mice via the JNK pathway. *Brain Research* **1359**, 216-226.

Li, P., Shen, M., Gao, F., Wu, J., Zhang, J., Teng, F. and Zhang, C. (2017) An antagomir to MicroRNA-106b-5p ameliorates cerebral ischemia and reperfusion injury in rats via inhibiting apoptosis and oxidative stress. *Molecular Neurobiology* **54**, 2901-2921.

Lv, C., Ma, Q., Han, B., Li, J., Geng, Y., Zhang, X. and Wang, M. (2018) Long-term DL-3-n-Butylphthalide treatment alleviates cognitive impairment correlate with improving synaptic plasticity in SAMP8 mice. *Frontiers in Aging Neuroscience* **10**, 200.

McGrath, J. C., Drummond, G. B., McLachlan, E. M., Kilkenny, C. and Wainwright, C. L. (2010) Guidelines for reporting experiments involving animals: the ARRIVE guidelines. *British Journal of Pharmacology* **160**, 1573-1576.

Minjarez, B., Camarena, H. O., Haramati, J., Rodríguez-Yañez, Y., Mena-Munguía, S., Buriticá, J. and García-Leal, O. (2017) Behavioral changes in models of chemoconvulsant-induced epilepsy: a review. *Neuroscience and Biobehavioral Reviews* **83**, 373-380.

Petersen, R. C., Parisi, J. E., Dickson, D. W., Johnson, K. A., Knopman, D. S., Boeve, B. F., Jicha, G. A., Ivnik, R. J., Smith, G. E., Tangalos, E. G., Braak, H. and Kokmen, E. (2006) Neuropathologic features of amnestic mild cognitive impairment. *Archives of Neurology* **63**, 665-672.

Qi, Q., Xu, J., Lv, P., Dong, Y., Liu, Z., Hu, M., Xiao, Y., Jia, Y., Jin, W., Fan, M., Zhang, D. and Meng, N. (2018) DL-3-n-butylphthalide alleviates vascular cognitive impairment induced by chronic cerebral hypoperfusion by activating the Akt/Nrf2 signaling pathway in the hippocampus of rats. *Neuroscience Letters* **672**, 59-64.

Singh, N., Saha, L., Kumari, P., Singh, J., Bhatia, A., Banerjee, D. and Chakrabarti, A. (2019) Effect of dimethyl fumarate on neuroinflammation and apoptosis in pentylenetetrazol kindling model in rats. *Brain Research Bulletin* **144**, 233-245.

Sun, B., Feng, M., Tian, X., Lu, X., Zhang, Y., Ke, X., Huang, S., Cao, J. and Ding, X. (2012) DL-3-n-Butylphthalide protects rat bone marrow stem cells against hydrogen peroxide-induced cell death through antioxidation and activation of PI3K-Akt pathway. *Neuroscience Letters* **516**, 247-252.

Teymournejad, O., Mobarez, A. M., Hassan, Z. M. and Talebi Bezmin Abadi, A. (2017) Binding of the Helicobacter pylori OipA causes apoptosis of host cells via modulation of Bax/Bcl-2 levels. *Scientific Reports* **7**, 8036.

Vossler, D. G., Weingarten, M. and Gidal, B. E. (2018) Summary of antiepileptic drugs available in the United States of America: working toward a world without epilepsy. *Epilepsy Currents* **18**, 1-26.

Wen, X. R., Tang, M., Qi, D. S., Huang, X. J., Liu, H. Z., Zhang, F., Wu, J., Wang, Y. W., Zhang, X. B., Guo, J. Q., Wang, S. L., Liu, Y., Wang, Y. L. and Song, Y. J. (2016) Butylphthalide Suppresses neuronal cells apoptosis and inhibits JNK-Caspase3 signaling pathway after brain ischemia /reperfusion in rats. *Cellular and Molecular Neurobiology* **36**, 1087-1095.

Yang, L., Kong, Y., Dong, X., Hu, L., Lin, Y., Chen, X., Ni, Q., Lu, Y., Wu, B., Wang, H., Lu, Q. R. and Zhou, W. (2019) Clinical and genetic spectrum of a large cohort of children with epilepsy in China. *Genetics in Medicine* **21**, 564-571.

Yang, W., Li, L., Huang, R., Pei, Z., Liao, S. and Zeng, J. (2012) Hypoxia inducible factor-1alpha mediates protection of DL-3-n-butylphthalide in brain microvascular endothelial cells against oxygen glucose deprivation-induced injury. *Neural Regeneration Research* **7**, 948-954.

Ye, J., Huang, Y., Que, B., Chang, C., Liu, W., Hu, H., Liu, L., Shi, Y., Wang, Y., Wang, M., Zeng, T., Zhen, W., Xu, Y., Shi, L., Liu, J., Jiang, H., Ye, D., Lin, Y., Wan, J. and Ji, Q. (2018) Interleukin-12p35 knock out aggravates doxorubicin-induced cardiac injury and dysfunction by aggravating the inflammatory response, oxidative stress, apoptosis and autophagy in mice. *EBioMedicine* **35**, 29-39.

Zhang, J., Xia, Y., Xu, Z. and Deng, X. (2016) Propofol suppressed hypoxia/reoxygenation-induced apoptosis in HBVSMC by regulation of the expression of Bcl-2, Bax, Caspase3, Kir6.1, and p-JNK. *Oxidative Medicine and Cellular Longevity* **2016**, 1518738.

Zhao, L. Z., Su, X. W., Huang, Y. J., Qiu, P. X. and Yan, G. M. (2003) Activation of c-Jun and suppression of phospho-p44/42 were involved in diphenylhydantoin-induced apoptosis of cultured rat cerebellar granule neurons. *Acta Pharmacologica Sinica* **24**, 539-548.